Differential Delay Between Two Geodetic GPS Receivers for L1 and L2 Code and Carrier Signals*

M. Hottovy, M. Weiss

***Abstract*—Differential delay measurements of two Global Positining System satellite signal receivers of different manufacture were measured without using geodetic processing software. The two receivers were connected to the same antenna through a splitter, and driven by the same clocks. We obtained the continuous averages of differential delays through the receivers over a period of 128 days. This report will describe the process by which we calculated these averages and will also present the results found for each of the four signal types studied, which are the L1 and L2 carrier phases, and the C1 and P2 code phases.**

I. Introduction

For the comparison of clocks using signals of Global Positioning System (GPS) [1] satellites, the total delay through the receiver and antenna system is critical. It is impossible to tell the difference between a change in this delay and the motion of the clock driving the receiver when comparing to a remote clock. To determine the relative stability of two receivers, we connected them through a splitter to the same antenna and antenna cable, as well as driving the receivers by the same clock. One receiver, NISA, was in a temperature controlled chamber. The other, NISV was open in the same room. We mention the manufacturers for information only. Neither endorsement nor criticism is implied. The NISA receiver was an Ashtech Z12T. The NISV receiver was a Novatel T-Sync receiver, with an OEM4 board.

II. Analysis Technique

The geodetic-type GPS receivers were connected with a splitter to the same antenna for 128 days. RINEX [2] files were stored with points taken every 30 seconds. Measurements were stored for the L1 and L2 carrier phases, and the C1 and P2 code phases. These data were used to obtain continuous averages of the differential delay through the two receivers for each of the four data types.

Initially, each type of data was differenced by taking NISA points from NISV points at matching reference times. This is what was used in computing the changes in differential delay. A satellite's pass started when there was at least half an hours' worth of carrier data in which there were no cycle slips between adjacent data points. A pass ended when either a cycle slip occurred or there was a break in reference time of two hours or greater.

For the code data, we found the average of the differences over all satellites tracked by both receivers at all reference times for which we had good data. This process gave the changes in differential receiver delay for each of the codes studied, C1 and P2.

The processing of the carrier data was not as simple since analysis was complicated by the differential cycle ambiguity between the two receivers. To account for this uncertainty, a constant was removed from each differenced data point in a satellite's pass before calculating the average. The constant was the first data point in the pass minus the current existing average. This entailed one constant per pass for every satellite for each of the L1 and L2 carrier phases. In this way the phase of a new satellite did not introduce a step in the average. The equations for the constants follow below.

Suppose, at time t_0, there is an existing average a_0, and a satellite j with its first data point p_{j0} of its pass. The data point p_{j0} is not used in computing a_0. Rather, we determine the constant c_{j0} as

$$c_{j0} = p_{j0} - a_0. \quad (1)$$

Now at times $t_n > t_0$, the average a_n was computed using the data p_{jn} for the N satellites, $j=1,\ldots,N$, that are in their respective same pass for which the constant c_{j0} was computed.

The equation is as follows

$$a_n = \sum (p_{jn} - c_{j0})/N. \quad (2)$$

The sum is over all satellites which are being tracked by both receivers at time t_n, starting with the first point after the constant c_{j0} has been determined. In this way a new satellite's difference was matched to the existing average, so that its addition to the averaging process caused no initial time step. Only the change in phase over a pass was used, since there was no absolute estimate of phase.

The carrier averaging process was initialized with the first average being the average of the cycle fraction of the initial satellites data present. This process gave the changes in differential delay over the 128 days through the two receivers for each of the GPS carriers, L1 and L2.

III. RESULTS

Fig. 1 shows the result of the analysis done on the L1 carrier data. It shows the change in differential delay over time between the two receivers. These results show that the differential delay increased from zero as time progressed, with some apparent linearity, though with sudden steps in some places. Fig. 2 expands a portion of Fig. 1 to illustrate a period of rapid change in the receivers' L1 carrier phase differential delay. The behavior around days 18 through 23 appears to have a period of about three times per day.

Analyzing the L2 carrier data yielded similar results, though with the differential delay decreasing. As we can see in Fig. 3, the averages computed for the L2 data behaved in the same manner, walking off from zero with several sudden changes along the way. Fig. 4 expands Fig. 3 illustrating anomalous periodic behavior in L2 data that also occur up to three times per day for days 18 through 23.

These variations must reflect the differential response to the received signals. It may have to do with how new satellites coming up over the horizon impact our averaging scheme. Except for cycle slips, we always computed the constant for the pass when the satellite was low on the horizon. We demand only that following the first point there are at least 30 minutes of data with no cycle slip. This combined with multi-path interference may explain some of the sharp variations., but does not explain why occur about three times per day.

The Time Deviation (TDEV) [3] plots of these results are shown in Fig. 5 and Fig. 6. TDEV in both data sets starts off at a magnitude of 2 to 3 ps at 120 s, and ends up at a magnitude of about 100 ps. The noise type is random-walk phase modulation (RWPM) from a few hundred seconds to 10^4 s, where we see a drop. This probably a diurnal periodic effect. After this we see another interval where RWPM dominates from 3 x 10^4 s out to about 1 d. Because our analysis technique involves an extension of an average to calibrate each additional satellite, a random-walk process in phase is natural.

However, there appears to be an underlying linear change in phase delay between the two receivers of order 2 ns in 100 d, increasing for L1 and decreasing for L2 data. Some of this may be due to the random walk process. TDEV at 10 d is about 100 ps. The expected phase deviation would be √3 times the TDEV values, continuing increase by the square root of the averaging time out to the data length. With the data length of order 100 d, we multiply 100 ps times √3 twice and obtain about 300 ps as potentially due to RWPM.

There are 19 intervals when we have no satellite data, primarily due to our editing. There are occasions where the receivers have no data, perhaps due to interference, such as lightning. An example of our editing is when a 30 s data point was missing in a period of data less than 30 minutes long, that whole period was not used. The minimum length of the intervals with no data used was 30 s and the maximum length was 47 minutes. Typical lengths were 30 s to a couple of minutes. Over these dead times, we simply carry forward the average from when we had satellites, to the arrival of the next satellite. This process would tend to exacerbate the random walk PM.

It would be convenient to blame the increase in offset on a random-walk process. However, it looks perhaps too linear for this. The approximate 2 ns change over 100 d, increasing with L1 data, decreasing with L2 corresponds to an error in frequency transfer of about 2×10^{-16}. This error would not enter into a transfer technique that used the code to estimate the cycle ambiguity of the carrier. If using a true carrier-only technique, with the ionosphere-free combination of 2.5xL1 + 1.5xL2 the frequency transfer error due to this underlying drift in the receiver carriers would be 8×10^{-16}. This would be a significant effect when using GPS carrier phase techniques to compare frequency standards whose uncertainties are below 1×10^{-15}. There is some evidence an effect like this may have been seen before in a comparison to Two-Way Satellite Time and Frequency Transfer [4].

In the end the offsets we found represents differential delays between the two receivers. The effects we know about that could cause this are the ones mentioned above: the RWPM, the different response to multi-path interference between the receivers, the fact that we calibrate the pass generally when the satellite is at a low angle, and finally a true change in delay between the receivers. Given that one receiver is temperature controlled, this might be a temperature coefficient between the receivers.

Fig. 7 shows the results of the differential delay computed for the C1 code data. The P2 code data results can be seen in Fig. 8. The outcome here did not show ramps as for the carrier data, as can be seen more clearly in Fig. 9 and Fig. 10, where we have low-pass filtered the data using a Kalman smoother. There are somewhat positive changes for C1 and generally negative for P2, over the period of study, but the magnitudes are much smaller. The effects do not appear to be linear. C1 appears to have jumps of about 0.2 ns over a few days. P2 seems to wander negative of order -0.1 ns over 100 d. Thus, this evidence suggests that a GPS carrier-phase time transfer

technique should use the code to resolve carrier ambiguity. While there may be some changes in delay occasionally that might be problematic, there is no evidence here of an on-going systematic that would impact frequency transfer at a level of a few parts in 10^{16}.

The TDEV values for the codes are shown in Fig. 11 and Fig. 12 for the C1 and P2 data, respectively. They start with the integration time of 120 s, since we averaged four points to reduce the processing load. The short term noise is consistent with a White PM model. The P2 level of 160 mps at 120 s is slightly better than the C1 level of 200 ps at 120 s, perhaps because of the higher chipping rate. However, the diurnal variation is somewhat worse for the P2. C1 has a TDEV of 40 ps at the almost half-day peak, whereas the P2 level is 120 ps. They both drop below 100 ps at one day, however.

IV. CONCLUSIONS

We studied the differential delays between two GPS geodetic receivers at NIST of different manufacture, NISV and NISA. We looked at the difference between the receivers' time stamps of the C1 and P2 codes, and the L1 and L2 phases. The differences between receiver times for the L1 and L2 phases changed in an apparent almost linear way by 2 ns over 100 d, with the L1 data increasing and the L2 data decreasing. This implies a potential limit in frequency transfer for a carrier-only GPS carrier frequency transfer of 8×10^{-16} for the ionosphere-free combination. The C1 and P2 code differences do not exhibit such a linear trend. However, there are some jumps in the C1 averages of 0.2 ns over a few days, and some bad points in the P2 data.

V. BIBLIOGRAPHY

[1] B.W. Parkinson, J.J. Spilker Jr., P. Axelrad, *Global Positioning System: Theory and Applications*, AIAA, 1996.

[2] W.Gurtner, G.M. Mader, "The RINEX format: current status, future developments," http://www.navcen.uscg.gov/pubs/gps/rinex/default.htm

[3] D.W. Allan, M.A. Weiss, and J.L. Jespersen, "A Frequency-Domain View of Time-Domain Characterization of Clocks and Time and Frequency Distribution Systems," Proc. 1991 IEEE Freq. Cont. Symp., pp.667-678, 1991.

[4] T.E. Parker, V.S. Zhang, A. McKinley, L.M. Nelson, J. Rohde, and D. Matsakis, "Investigation of Instabilities in Two-Way Satellite Time and Frequency Transfer," Proc. 2002 PTTI Mtg., pp.381-390, 2002.

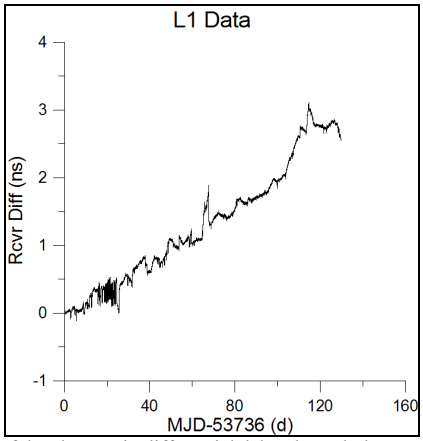

Fig. 1. Plot of the changes in differential delay through the two receivers for the GPS carrier L1. The delay is measured in nanoseconds and is plotted against MJD for the 128 day period.

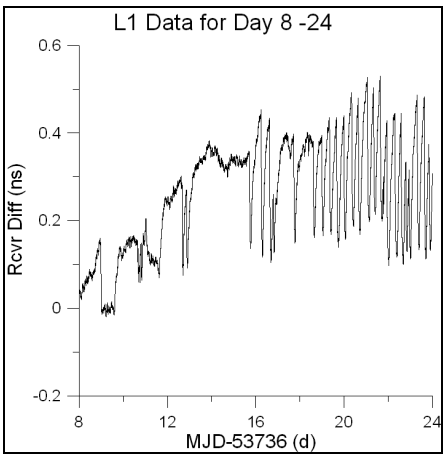

Fig. 2. Expanded view of Fig. 1 showing an example of the sudden jumps that occur in the changes in differential delay for the GPS carrier L1.

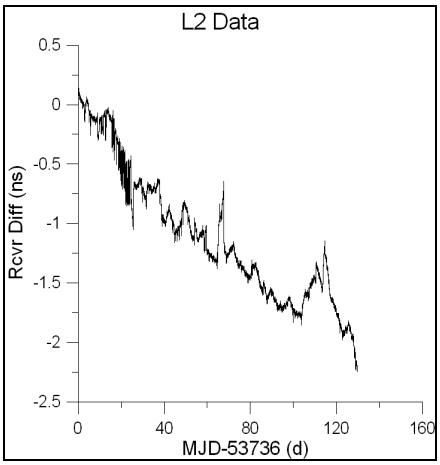

Fig. 3. Plot of the changes in differential delay through the two receivers for the GPS carrier L2. The delay is measured in nanoseconds and is plotted against MJD for the 128 day period.

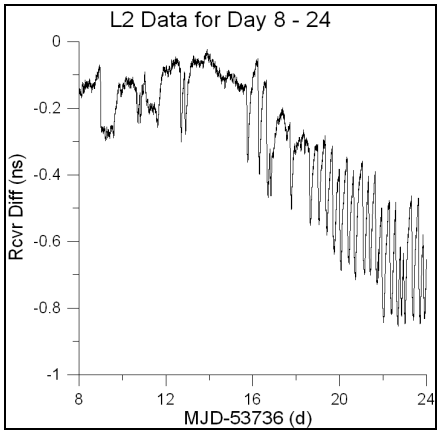

Fig. 4. Expanded view of Fig. 2 showing an example of the sudden jumps that occur in the changes in differential delay for the GPS carrier L2.

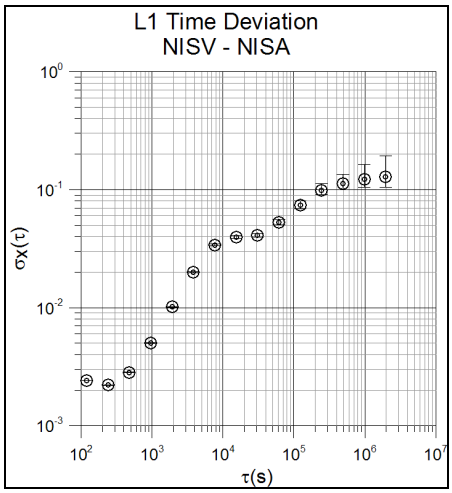

Fig. 5. Plot of the Time Deviation of the L1 averaged NISV-NISA data.

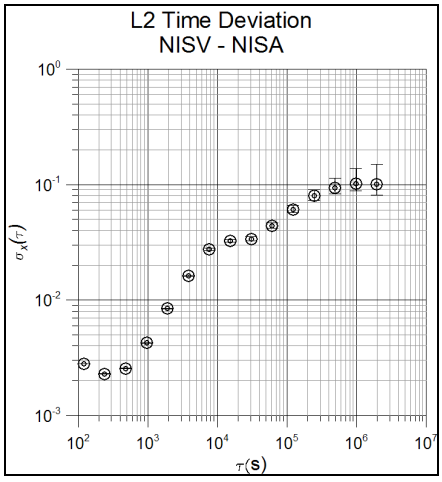

Fig. 6. Plot of the Time Deviation of the L2 averaged NISV-NISA data.

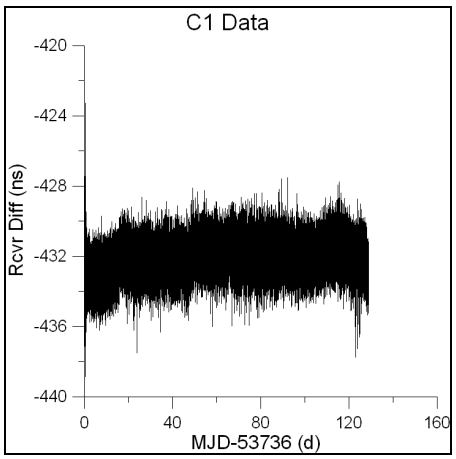

Fig. 7. Plot of the changes in differential delay through the two receivers for the GPS code C1. The delay is measured in nanoseconds and is plotted against MJD for the 128 day period.

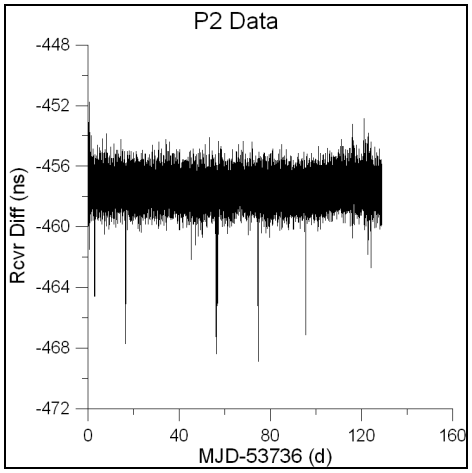

Fig. 8. Plot of the changes in differential delay through the two receivers for the GPS code P2. The delay is measured in nanoseconds and is plotted against MJD for the 128 day period.

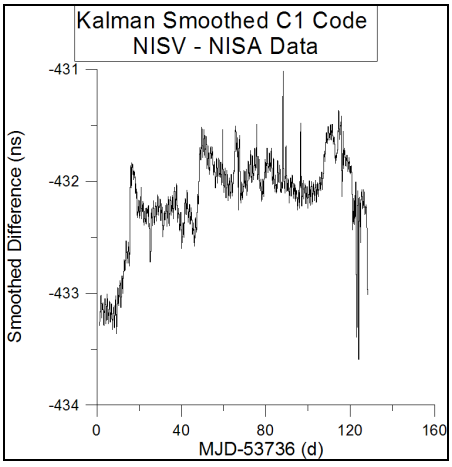

Fig. 9. Plot of the Kalman Smoothed C1 code averaged data, showing the lack of slope as in the L1 carrier phase data.

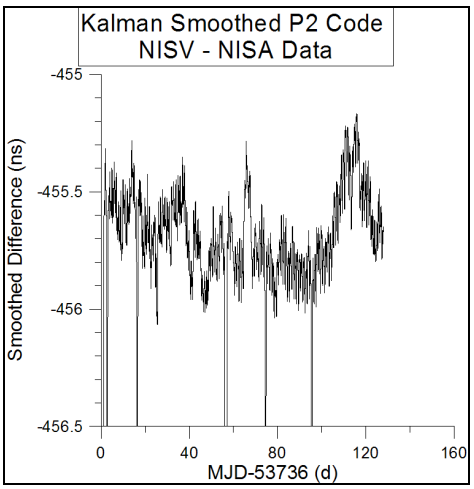

Fig. 10. Plot of the Kalman Smoothed P2 averaged data, showing the lack of slope as in the L2 data. The plot is clipped with a minimum of -456.5 ns due to some apparent bad data points.

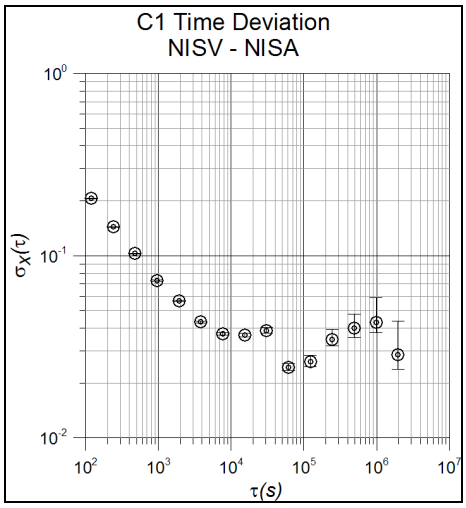

Fig. 11. Plot of the Time Deviation of the C1 averaged data.

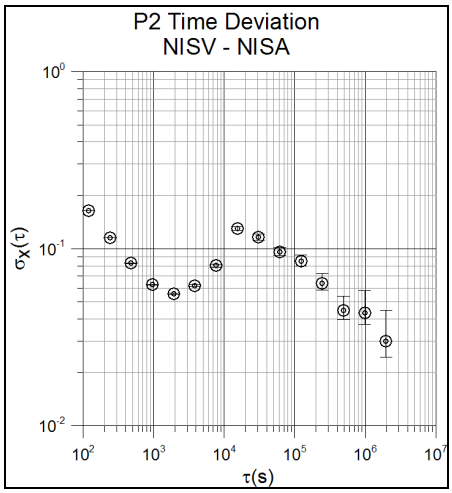

Fig.12. Plot of the Time Deviation of the P2 averaged data.